International Journal of Pharmaceutics 360 (2008) 213–218

Contents lists available at ScienceDirect

International Journal of Pharmaceutics

journal homepage: www.elsevier.com/locate/ijpharm

Pharmaceutical Nanotechnology

Dissolution-rate enhancement of fenofibrate by adsorption onto silica using supercritical carbon dioxide

Ganesh P. Sanganwar, Ram B. Gupta*

Department of Chemical Engineering, Auburn University, Auburn, AL 36849, USA

ARTICLE INFO

Article history:
Received 6 January 2008
Received in revised form 22 April 2008
Accepted 23 April 2008
Available online 4 May 2008

Keywords:
Fenofibrate
Silica
Supercritical carbon dioxide
Dissolution-rate enhancement
Adsorption
Poorly water-soluble drugs

ABSTRACT

Dissolution rate of a poorly water-soluble drug, fenofibrate, is increased by adsorbing the drug onto silica. The adsorption is achieved by first dissolving the drug in supercritical carbon dioxide and then depressurizing the solution onto silica. Loadings of up to 27.5 wt.% drug onto silica are obtained. Since solvents are not used in the loading process, the fenofibrate/silica formulation is free of any residual solvent, and carbon dioxide is freely removed upon depressurization. The formulation is characterized using infrared spectroscopy, ultraviolet spectroscopy, X-ray diffraction, differential scanning calorimetry and scanning electron microscopy. Based on *in vitro* dissolution study, a significant increase in the dissolution rate (~80% drug release in 20 min) of drug–silica formulation is observed as compared to micronized fenofibrate (~20% drug release in 20 min), which can be attributed to increase in the surface area and decrease in the crystallinity of drug after adsorption onto silica. Two different formulations are compared: (A) amorphous fenofibrate/silica and (B) slightly crystalline fenofibrate/silica. The second formulation is found to be more stable on storage.

1. Introduction

Bioavailability of poorly water-soluble hydrophobic drugs [Class II in Biopharmaceutics Classification System] is limited by their solubility and dissolution rate (Amidon et al., 1995). The dissolution rate of these drugs can be improved by decreasing particle size, decreasing crystallinity, and/or increasing the surface area. Several studies have been carried out to increase the dissolution rate of drugs by decreasing the particle size, by creating nano- and micro-particles (Liversidge and Cundy, 1995; Jounela et al., 1975; Rasenack and Muller, 2002). However, the fine drug particles have high tendency to agglomerate due to van der Waals attraction or hydrophobicity, which both result in a decrease in surface area over time (Finholt and Slovang, 1968; Aguiar et al., 1967). Another way of increasing the dissolution rate is adsorption of the drug onto a high-surface-area carrier. In this technique, the drug is dissolved in an organic solvent (e.g., methanol, acetone, methylene chloride) followed by soaking of the solution by a high-surface-area carrier such as silica (Friedrich et al., 2006; Charnay et al., 2004; Heikkila et al., 2007; Monkhouse and Lach, 1972a; McGinity and Harris, 1980). Here, agglomeration of the drug particles is prevented due to the binding of drug to the carrier. However, due to the presence of the residual solvent in the drug formulation, it is disadvantageous to use toxic solvents. To overcome the problem, supercritical carbon dioxide, which is non-toxic and non-flammable, is used as a solvent to adsorb drug onto high surface area carriers (Smirnova et al., 2004).

Supercritical fluids have liquid-like densities and gas-like diffusivities. Out of various supercritical fluids, carbon dioxide is suitable for processing of pharmaceutical compounds due to its mild critical point (73.7 bar and 31.1 °C). Also, small non-polar or hydrophobic molecules can be easily solubilized in CO_2 which is in relatively non-polar, and the solubility can be adjusted with the CO_2 density (Gupta and Shim, 2007). Also, due to the high molecular diffusivity, the drug can be easily transported to the carrier nanopores. Upon depressurization, CO_2 leaves the solid matrix without any residues.

In this study, adsorption of fenofibrate through supercritical CO_2 onto silica was carried out for dissolution enhancement. Till now, there have been several studies to increase dissolution of fenofibrate, for example, (a) complexing with cyclodextrin (Aigner et al., 1995; Patel and Vavia, 2006), (b) solid dispersion in PEG and PVP (Sheu et al., 1994), and (c) micronization (Munoz et al., 1994; Vogt et al., 2008). However, no attempt was made to adsorb fenofibrate onto a high-surface-area carrier. Also, it is interesting to study the adsorption of fenofibrate onto high-surface-area carrier due to the low glass transition temperature (−20 °C) of the drug.

Fenofibrate (2-[4-(4-cholrobenzyol) phenoxy]-2-methyl-propanoic acid, 1-methylsethyl ester) is hydrophobic/lipophilic (MW = 360.831 g/mol, log P = 5.575; Wishart et al., 2006) drug with negligible solubility in water (Munoz et al., 1994). Bioavailability

* Corresponding author. Tel.: +1 334 844 2013; fax: +1 334 844 2063.
E-mail address: gupta@auburn.edu (R.B. Gupta).

0378-5173/$ – see front matter © 2008 Elsevier B.V. All rights reserved.
doi:10.1016/j.ijpharm.2008.04.041

of fenofibrate solely depends on dissolution rate in the gastrointestinal tract. This drug is used in lipid regulation as it decreases low-density lipoprotein (LDL) and very-low-density lipoprotein (VLDL) levels, and increases high-density lipoprotein (HDL) level.

Non-porous fumed silica has been used in oral formulation as glidant, and as a carrier (Monkhouse and Lach, 1972b). We have utilized pharmaceutical grade fumed silica consisting of 200–300 nm long aggregates of 9–30 nm size primary nanoparticles. This silica also forms 30–44 μm size macro-agglomerates with a very high (>98%) void volume (Cabot Corp., 2007a,b,c). The hydrophilic silica adsorbs moisture therefore can be used in moisture sensitive drug formulations. Also, hydroxyl groups located on siloxane surface can hydrogen bond with drug molecule providing additional interaction (Madieh et al., 2007).

2. Materials and method

2.1. Materials

Fenofibrate (>99% pure, Sigma–Aldrich), CAB-O-SIL M-5P fumed silica ($200 \pm 15\ m^2/g$ surface area, 40 g/l tapped density, Cabot, Inc.), dichloromethane (99.9% pure, Sigma–Aldrich), sodium chloride (ACS grade, Fisher Scientific), sodium dodecyl sulfate (>99% pure, Sigma–Aldrich), hydrochloric acid (ACS grade, Fisher Scientific), methanol (>99.9% pure, Fisher Scientific), and CO_2 (bone dry, Air Gas) were used as received.

2.2. Adsorption of drug onto silica

Fig. 1 shows a schematic of the experimental setup used for adsorption of a drug onto silica. Silica is sealed in a porous Whatmann filter paper (11 μm pore size) pouch and kept inside the pressure vessel (V, 100 ml) containing an excess amount of fenofibrate. CO_2 is pumped inside the pressure vessel to the desired pressure (2550 ± 50 psig) and temperature is maintained (40 or $50 \pm 0.1\ ^\circ C$) using a heating tape. The content is allowed to equilibrate for 150 min at a constant pressure and temperature. Afterwards, the vessel is slowly depressurized over 4 h to remove CO_2, after which the silica–fenofibrate formulation is collected from the filter paper pouch. Experiments are repeated to obtain sufficient amount of the formulation needed for analyses; the formulations are mixed before further analyses. Drug loading (g drug/g silica–drug formulation) was measured by dissolving a known amount of the formulation into methanol, followed by concentration analysis using UV spectroscopy at 287 nm. Weight measurements are done at 50% relative humidity (air conditioned laboratory), to avoid moisture uptake by hydrophilic silica which usually occurs at >70% relative humidity.

2.3. Fourier transform infrared spectroscopy (FT-IR spectroscopy)

Infrared spectra of the samples were obtained using Avatar 360 FT-IR (Nicolet). The formulation sample was mixed with 100 fold KBr for preparing the tablets. The final spectra are composed of 64 scans performed in range of 400–4000 cm^{-1} with 2 cm^{-1} resolution.

2.4. Powder X-ray diffraction

Crystallinity of the formulation was analyzed using the Rigaku X-ray diffractometer which is equipped with a Cu $K\alpha_1$ radiation source at 40 kV voltage, 40 mA current and a miniflex gonoiometer. Diffraction patterns were obtained in 2θ range of 10–80° using 0.05° step size and 5°/min scan speed.

2.5. Differential scanning calorimetry (DSC)

DSC analysis (thermograph) of samples was done using TA Instruments, model DSC Q2000. 1–4 mg samples were weighed in aluminum pans and analyzed with heating rate of 5 °C/min over the temperature range of 20–100 °C. Degree of crystallinity (X) was determined from calorimetric data as follows (Pikal et al., 1978)

$$X = \frac{(\Delta H_s - \Delta H_a)}{(\Delta H_c - \Delta H_a)} \times 100(\%) \quad (1)$$

where ΔH_s, ΔH_a, and ΔH_c are the heats of fusion for actual, completely amorphous, and completely crystalline formulations, respectively.

2.6. Scanning electron microscopy (SEM)

Surface morphologies of the drug and drug–silica formulation were studied using field emission scanning electron microscope (JEOL 7000 F). The sample is blown onto adhesive carbon tape on aluminum stub followed by sputter coating of gold.

2.7. Saturation solubility

Saturation solubility of fenofibrate was obtained by intense stirring (using wrist action shaker) excess amount of drug in 10 ml of 0.1N HCl containing 0.3% (w/v) sodium dodecyl sulfate and 0.2%

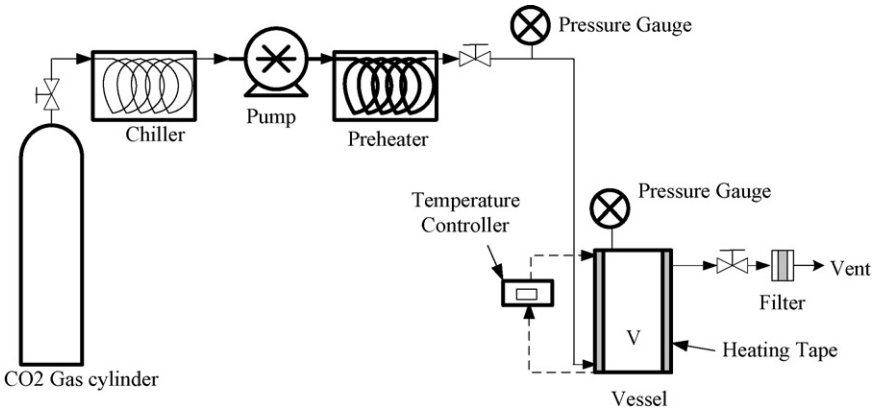

Fig. 1. Schematic of supercritical CO_2 apparatus for drug adsorption onto silica.

(w/v) NaCl at 23 °C for 8 h. Sample was filtered using 200 nm inline syringe filter (PTFE, 17 mm, Alltech) to remove any suspended particles. UV absorbance of sample was measured at 287 nm after appropriate dilution.

2.8. Drug dissolution

Drug dissolution was carried out by placing sample (equivalent to 7 mg of drug) in 400 ml freshly prepared 0.1N HCl solution (pH 1.2 ± 0.1) containing 0.3% (w/v) sodium dodecyl sulfate and 0.2% (w/v) NaCl at 37 °C (U.S. Department of Health, 2007a) in a horizontal shaker (Environ Shaker, Lab-line Instruments) at 100 rpm. Although dissolution data obtained using a USP dissolution apparatus (or method) can be easily compared with the data for other formulations in the literature, but the fundamental conclusion on the efficacy of the supercritical fluid technique is still valid with the dissolution method used here. Similar kind of horizontal shaker has been used by Friedrich et al. (2006) to study drug dissolution. The ratio of drug saturation concentration to actual drug concentration in dissolution media was 4 (at 23 °C) which is more than 3-fold required for maintaining desired sink condition while conducting dissolution experiments (USP 28, 2005). 2 ml samples were drawn at time interval of 10, 20, 30, 45, 60, 75, and 90 min. Change in volume of solution due to sample withdrawal was considered during concentration determinations. Samples were filtered using 200 nm inline syringe filter (PTFE, 17 mm, Alltech) to remove any suspended particles. Drug concentrations were measured using UV spectroscopy (Spectronic Genesys 2) at 287 nm. The measurements were done in duplicate and averages are reported here.

2.9. Physical stability

For stability analysis, a known amount of fenofibrate–silica formulation was kept in a capped glass vial at 40 °C and 75% relative humidity (U.S. Department of Health, 2007b). Desired humidity was maintained using saturated NaCl solution. After 1 month, the samples were tested for drug release and crystallinity.

3. Result and discussion

3.1. Loading of drug onto silica

Loading of fenofibrate onto silica was carried out at two temperatures: 40 and 50 °C. The loading of 27.5 wt.% drugs onto silica (formulation A) was obtained at 2550 psig and 40 °C (CO_2 density, 0.82 g/ml) while drug loading of 25 wt.% (formulation B) was obtained at 2550 psig and 50 °C (CO_2 density, 0.75 g/ml). The variation in the drug loading was achieved from the phenomenon that the drug solubility in supercritical density depends upon the CO_2 density.

3.2. Infrared spectroscopy

State of drug molecule onto surface of silica was determined using FT-IR. Fig. 2 shows IR spectra of physical mixture of fenofibrate and silica and fenofibrate adsorbed onto silica. Characteristic intensity peaks for fenofibrate and silica have been reported by Lin-Vien et al. (1991). IR-spectra of physical and loaded mixtures are exactly the same, and there is no shift of peaks after adsorption of drug onto silica surface; indicating that there is no change in chemical structure of drug after loading onto silica. Specific fenofibrate peaks are observed at 2990, 1740, 1660, and 1600 cm^{-1} both in physical mixture of silica and fenofibrate and silica–fenofibrate formulation.

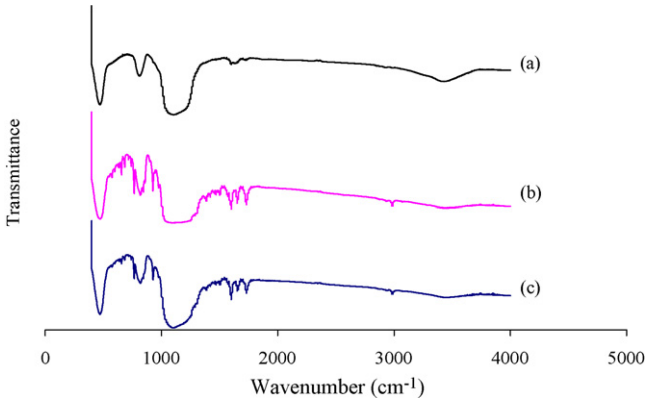

Fig. 2. FTIR spectra of (a) silica, (b) physical mixture of fenofibrate and silica, and (c) fenofibrate adsorbed onto silica formulation.

3.3. Crystallinity

Fig. 3 shows the XRD patterns for silica, fenofibrate and silica–fenofibrate formulation. Fenofibrate crystals show various diffraction peaks due to its crystalline structure. However, silica does not show any peak due to its amorphous nature. Fig. 3b shows a loss of drug crystallinity for formulation A due to drug loading onto silica surface. In formulation B, a few less intense and wide diffraction peaks of fenofibrate are observed, which can be attributed to the adsorption process in which some of amorphous drug may have crystallized due to higher temperature (50 °C). In fact, Zhou et al. (2002) reported that at temperature higher than 40 °C [i.e., above $(T_c - T_g)/T_m - T_g)$ value of 0.6, where, T_c is crystallization temperature (40 °C), T_g is glass transition temperature (−20 °C), and T_m is melting point (80.5 °C)], the molecular mobil-

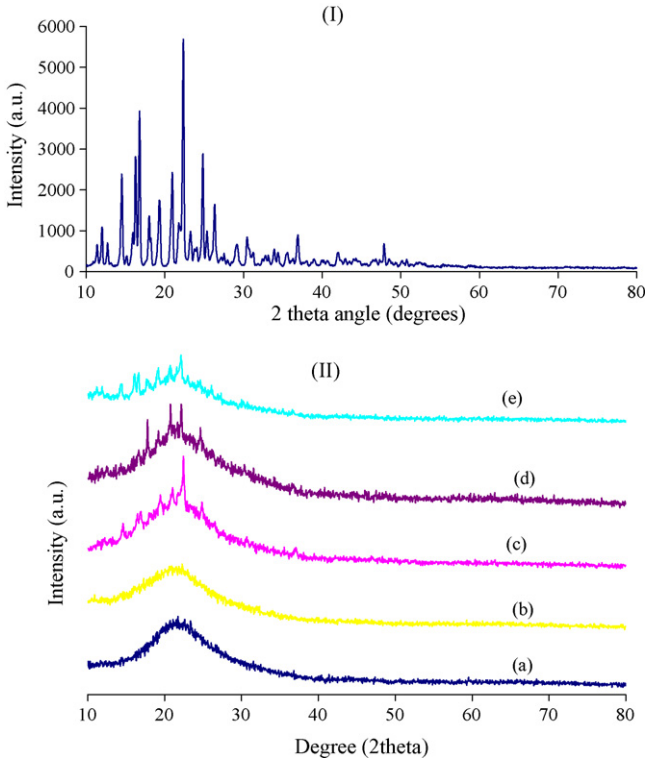

Fig. 3. XRD of (I) crystalline fenofibrate, and (II) (a) silica, (b) formulation A, (c) formulation B, (d) formulation A after 1 month storage, and (e) formulation B after 1 month storage.

Table 1
Melting point depression, heat of fusion, and degree of crystallinity for fenofibrate and fenofibrate–silica formulations

Formulation	Melting point depression (°C)	Heat of fusion (J/g)	Degree of crystallinity (%)
Fenofibrate (micronized, from supplier)	0 (T_m = 81.27 °C)	94.78	100
Fenofibrate–silica (physical mixture)	0.73	33.70	–
Formulation A	2.48	10.11	0 (completely amorphous)
Formulation B	2.26	9.83	4.4
Formulation A after 1 month storage	1.83	5.21	–
Formulation B after 1 month storage	2.19	12.24	21.0

ity of fenofibrate becomes exponentially high, resulting in a high probability of spontaneous crystallization.

3.4. DSC study

DSC thermographs for fenofibrate, physical mixture [0.72:0.28 (w/w)] of silica and fenofibrate, and fenofibrate–silica formulation were obtained. The corresponding melting point depressions, enthalpy of fusion, and degree of crystallinity are shown in Table 1. A depression in melting point of fenofibrate was found for physical mixture with silica, which indicates an interaction of silica with similar to observations by Wang et al. (2006) and Madieh et al. (2007). Decrease in melting point depression for formulations A and B upon storage is due to increase in crystallinity of formulation. The DSC thermograph for fenofibrate–silica formulation A shows only endothermic peak; the absence of exothermic recrystallization peak may be attributed to interaction between silica and drug, similar to observations of Vogt et al. (2008). Based on XRD data, formulation A was assumed to be completely amorphous and its enthalpy data was used for calculation of degree of crystallinity.

For formulation B, the degree of crystallinity was found to increase from 4 to 21% upon storage. While in the case of formulation A, decrease in enthalpy of fusion upon storage could not be explained. For physical mixture, crystallinity cannot be accurately determined as it is difficult to have a homogenous sample of 4 mg which was used for DSC analysis. Though, Wang et al. (2006) have observed that the crystallinity decreases after physically mixing with silica.

3.5. Morphology

Fig. 4a and b shows the spongy structure of silica–fenofibrate formulation without any crystals of fenofibrate due to the agglomeration of silica nanoparticles. Since fenofibrate is adsorbed on to surface of silica, there is no change in morphological structure of silica.

3.6. Saturation solubility

In this study, solubility of fenofibrate was found to be ~70 μg/ml as compared to literature value of ~92 μg/ml (Jamzad and Fassihi, 2006).

3.7. Dissolution

Fig. 5 shows the dissolution profile for fenofibrate (crystalline, micronized) and for both the fenofibrate–silica formulations. Dissolution of fenofibrate adsorbed onto silica (fenofibrate–silica formulation) was substantially higher (~80% drug release in 20 min) than that of micronized fenofibrate (~18% drug release in 20 min). Drug dissolution of 90% was obtained in 30 min for drug–silica formulation, whereas complete (100%) dissolution of fenofibrate was observed within 24 h. The high dissolution rate of fenofibrate–silica formulation can be attributed to an increase in the surface area of fenofibrate after adsorption onto silica, and a good wetting due to the hydrophilic nature of silica. In general, the amorphous structure of hydrophobic compound has higher dissolution rate than the crystalline compound, in aqueous media (Corrigan and Holohan, 1984; Froster et al., 2001). Dissolution profiles for formulation A and formulation B are almost similar even though fenofibrate–silica formulation obtained at 50 °C (formulation B) shows some degree of crystallinity as shown in Fig. 3c due to the formation of nanocrystals from amorphous drug at loading conditions of 50 °C. Fraction drug release (F) versus time (t) data was fitted to three different dissolution models: (1) Higuchi [$F = k_h t^{0.5}$], (2) Korsmeyer–Peppas [$F = k_p t^n$], and (3) Hixson-Crowell cube root [$F = 1 - (1 - k_b t)^3$] (Costa and Lobo, 2001). The model constants obtained from release profiles data are given in Table 2. The Korsmeyer–Peppas and Hixson–Crowell models accurately correlate the dissolution of fenofibrate. A value of n = 0.765

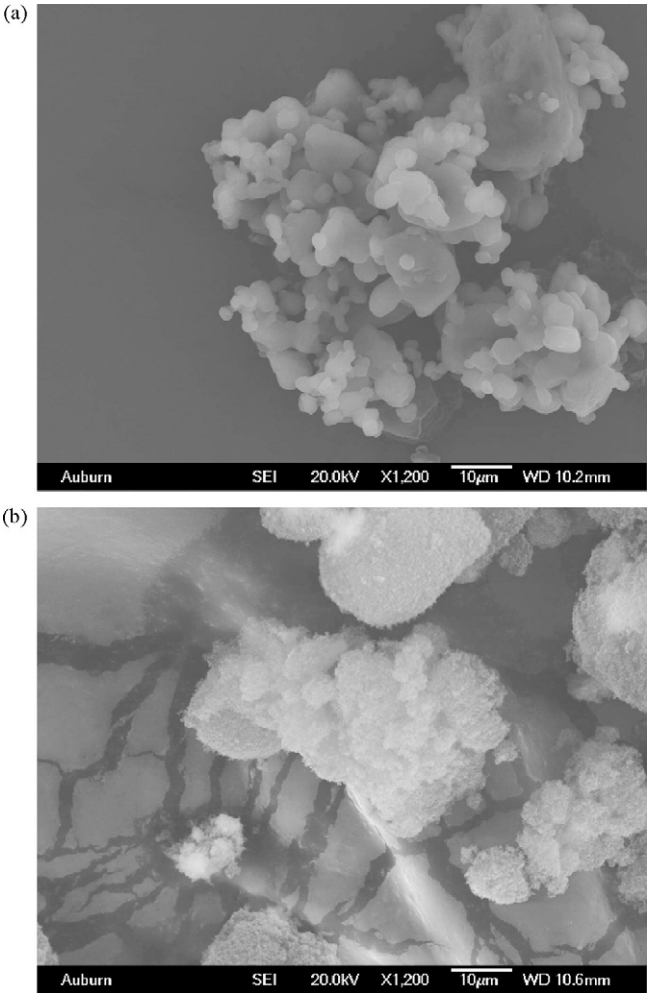

Fig. 4. SEM micrographs of (a) microcrystalline fenofibrate, and (b) fenofibrate adsorbed onto silica.

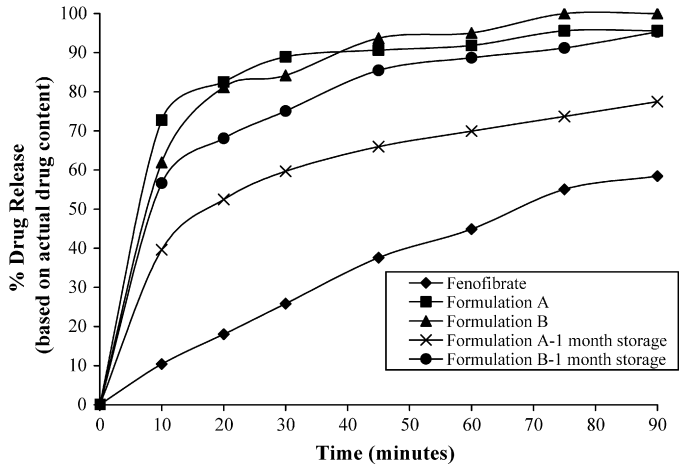

Fig. 5. Dissolution profiles of fenofibrate and fenofibrate–silica formulations.

for the Korsmeyer–Peppas model indicates anomalous transport of drug (i.e., non-fickian mass transfer) in pure drug dissolution. Korsmeyer–Peppas model is applicable to initial 60% release of drug; therefore, dissolution constants for silica–fenofibrate formulation were not obtained due to absence of more readings for drug release between 0 to 60%. Good fit for dissolution rate of fenofibrate–silica formulation could not be obtained with aforementioned dissolution models, indicating the deviation from the models.

3.8. Physical stability

High-energy, amorphous form of drugs may be unstable during storage due to a high tendency to transform into a more stable crystalline form having lower energy (Kaushal et al., 2004; Hancock and Zorafi, 1997). Fenofibrate has a low glass transition temperature of −20 °C; therefore, it will have a high tendency (due to a high molecular mobility) to crystallize at ambient storage conditions, which can reduce the dissolution rate. However, specific fenofibrate–silica H-bonding interaction can prevent the crystallization of drug during storage conditions. Fig. 5 shows the dissolution profiles for the fenofibrate–silica formulations stored for 1 month at 40 °C and 75% relative humidity. During the storage, a significant decrease in the dissolution rate of formulation A (Fig. 5, only ∼50% drug release in 20 min) is observed due to crystallization of amorphous fenofibrate (Fig. 3d; sharp crystalline fenofibrate peaks are observed.). Melting point data from DSC thermograph (Table 1) also shows increase in melting temperature for formulation A after 1 month storage as compared to initial amorphous formulation. Upon crystallization during storage, drug particles may have grown in size due to multilayer adsorption of drug onto surface of silica, which results in a decrease in surface area. According to Noyes–Whitney equation, dissolution rate is proportional to surface area (with rest of parameters being constant). Using density of fenofibrate as ∼0.9 g/ml, the thickness of drug molecule layer can be calculated from wt.% drug loading, surface area of silica, and a approximate width of a single fenofibrate molecule as 5 Å (Jmol, 2007 and Wishart et al., 2006). The thickness of drug layer was calculated as 12.5 Å for formulation A and 11.3 Å for formulation B. indicating that formulation B has less number of drug molecules available for growth during storage than for formulation A. Growth of drug molecules can be confirmed by comparing DSC thermograph (melting temperature, Table 1) for both the formulations after 1 month storage. For formulation B, dissolution rate was only slightly changed due to increase in crystallinity upon storage (∼68% drug release in 20 min, and ∼95% drug release in 90 min), which is consistent with no substantial differences between the X-ray diffraction patterns [Fig. 3c and e]. Hence, fenofibrate–silica formulation B is more stable than formulation A, which may be due to the fact that formulation B already has some crystallinity upon production.

Table 2
Dissolution-rate constants from three dissolution models

Compound	Higuchi		Korsmeyer–Peppas			Hixson–Crowell	
	K_h	R^2	K_{kp}	R^2	n	K_{hc}	R^2
Fenofibrate	0.057	0.934	0.019	0.994	0.765	0.003	0.994
Formulation A	0.13	0.59	–	–	–	0.016	0.79
Formulation B	0.128	0.76	–	–	–	0.016	0.91

4. Conclusion

Adsorption of fenofibrate on high-surface-area silica significantly increases the drug dissolution rate. In addition, the adsorption of fenofibrate from supercritical carbon dioxide does not leave any residual solvent in the final formulation. Amorphous drug–silica formulation obtained using CO_2 at 2550 psig and 40 °C is found to be unstable during storage due to crystallization. On the other hand, slightly crystalline drug–silica formulation obtained using CO_2 at 2550 psig and 50 °C is found to be stable during storage.

Acknowledgments

Financial support from National Science Foundation through NIRT grant DMI-0506722 and experimental assistance from Andrew Scott (a NSF REU student for site 0552557) are highly appreciated.

References

Aguiar, A.J., Zelmer, A.W., Kinkel, A.W., 1967. Deaggregation behavior of a relatively insoluble substituted benzoic acid and its sodium salt. J. Pharm. Sci. 56, 1243–1252.
Aigner, Z., Bencz, I., Kata, M., 1995. Increasing the solubility characteristics of fenofibrate with cyclodextrin. J. Inclusion Phenomena Mol. Recognit. Chem. 20, 1–252.
Amidon, G.L., Lennernas, H., Shah, V.P., Crison, J.R., 1995. A theoretical basis for a biopharmaceutical drug classification: the correlation of in vitro drug product dissolution and in vivo bioavailability. Pharm. Res. 12, 413–420.
Cabot Corp., 2007. Applications of CAB-O-SIL M-5P fumed silica in formulation and design of solid dosage forms. Available via www.cabot-corp.com (accessed on June 20, 2007).
Cabot Corp., 2007. Functions of CAB-O-SIL fumed silica in pharmaceutical applications. Available via www.cabot-corp.com (accessed on June 20, 2007).
Cabot Corp., 2007. Properties of CAB-O-SIL M-5P fumed silica. Available via www.cabot-corp.com (accessed on June 20, 2007).
Charnay, C., Begu, S., Tourne-Peteilh, C., Nicole, L., Lerner, D.A., Devoisselle, J.M., 2004. Inclusion of ibuprofen in mesoporous templated silica:drug loading and release property. Eur. J. Pharm. Biopharm. 57, 533–540.
Corrigan, O.I., Holohan, E.M., 1984. Amorphous spray-dried hydroflumethiazide-polyvinylpyrrolidone systems: physicochemical properties. J. Pharm. Pharmacol. 36, 217–221.
Costa, P., Lobo, J.M.S., 2001. Modeling and comparison of dissolution profiles. Eur. J. Pharm Sci. 13, 123–133.
Finholt, P., Slovang, S., 1968. Dissolution kinetics of drugs in human gastric juice the role of surface tension. J. Pharm. Sci. 57, 1322–1326.
Friedrich, H., Fussnegger, B., Kolter, K., Bodmeier, R., 2006. Dissolution rate improvement of poorly water soluble drugs obtained by adsorbing solutions of drugs in solvents onto high surface area carriers. Eur. J. Pharm. Biopharm. 62, 171–177.
Froster, A., Hempenstall, J., Rades, T., 2001. Characterization of glass solutions of poorly water-soluble drugs produced by melt extrusion with amorphous polymers. J. Pharm. Pharmacol. 53, 303–315.
Gupta, R.B., Shim, J.J., 2007. Solubility in Supercritical Carbon Dioxide. Taylor and Francis Group, New York.
Hancock, B.C., Zorafi, G., 1997. Characteristics and significance of the amorphous state in pharmaceutical systems. J. Pharm. Sci. 86, 1–12.
Heikkila, T., Salonen, J., Tuura, J., Hamdy, M.S., Mul, G., Kumar, N., Salmi, T., Murzin, D.Yu., Laitinen, L., Kaukonen, A.M., Hirvonen, J., Lehto, V.-P., 2007. Mesoporous silica material TUD-1 as drug delivery system. Int. J. Pharm. 331, 133–138.

Jamzad, S., Fassihi, R., 2006. Role of surfactant and pH on dissolution properties of fenofibrate and glipizide-technical note. AAPS Pharm. Sci. Tech. 7, E1–E6.
Jmol. An open-source java viewer for chemical structures in 3D. Available via http://jmol.sourceforge.net/ (accessed on August 15, 2007).
Jounela, A., Pentikainen, P., Sothmann, A., 1975. Effect of particle size on the bioavailability of digoxin. Eur. J. Clin. Pharmacol. 8, 365–370.
Kaushal, A.M., Gupta, P., Bansal, A.K., 2004. Amorphous drug delivery systems: molecular aspects, design, and performance. Crit. Rev. Ther. Drug Carrier Syst. 21, 133–193.
Lin-Vien, D., Colthup, N.B., Fateley, W.G., Grasselli, J.G., 1991. The Handbook of Infrared and Raman Characteristic Frequencies of Organic Molecule. Academic Press Inc., San Diego.
Liversidge, G.G., Cundy, K.C., 1995. Particle size reduction for improvement of oral bioavailability of hydrophobic drugs: absolute oral bioavailability of nanocrystalline danzol in beagle dogs. Int. J. Pharm. 125, 91–97.
Madieh, S., Simone, M., Wilson, W., Mehra, D., Augsburger, L., 2007. Investigation of drug-porous adsorbent interactions in drug mixtures with selected porous adsorbents. J. Pharm. Sci. 96, 851–863.
McGinity, J.W., Harris, M.R., 1980. Increasing dissolution rates of poorly soluble drugs by adsorption to montmorillonite. Drug Dev. Ind. Pharm. 6, 35–48.
Monkhouse, D.C., Lach, J.L., 1972a. Use of adsorbents in enhancement of drug dissolution I. J. Pharm. Sci. 6, 1430–1435.
Monkhouse, D.C., Lach, J.L., 1972b. Use of adsorbents in enhancement of drug dissolution II. J. Pharm. Sci. 6, 1435–1441.
Munoz, A., Guichard, J.P., Reginault, Ph., 1994. Micronized fenofibrate. Atherosclerosis 110, S45–S48.
Patel, A.R., Vavia, P.R., 2006. Effect of polymer on solubilization of fenofibrate by cyclodextrin complexation. J. Inclusion Phenomena Macrocyclic Chem. 56, 247–251.
Pikal, M.J., Lukes, A.L., Lang, J.E., Gaines, K., 1978. Quantative crystallinity determinations for β-lactam antibiotics by solution calorimetry: correlation with stability. J. Pharm. Sci. 67, 767–773.
Rasenack, N., Muller, B.W., 2002. Dissolution rate enhancement by in situ micronization of poorly water-soluble drugs. Pharm. Res. 19, 1894–1900.
Sheu, M.T., Yeh, C.M., Sokoloski, T.D., 1994. Characterization and dissolution of fenofibrate solid dispersion systems. Int. J. Pharm. 103, 137–146.
Smirnova, I., Suttiruengwong, S., Seiler, M., Arlt, W., 2004. Dissolution rate enhancement by adsorption of poorly soluble drugs on silica aerogels. Pharm. Dev. Tech. 9, 443–452.
U.S. Department of Health and Human Services Food and Drug administration. Guidance for industry Q1A stability testing of new drug substances and products. Available via http://www.fda.gov/cder/guidance/index.htm (accessed on June 20, 2007).
U.S. Department of Health and Human Services Food and Drug administration. Guidance for industry. Dissolution testing of immediate release solid oral dosage forms. Available via http://www.fda.gov/cder/Guidance/1713bp1.pdf (accessed on June 20, 2007).
United States Pharmacopeial Convention, 2005. In Vitro and In Vivo Evaluation of Dosage Forms. United States Pharmacopeial Convention Inc., USP 28, Rockville, MD, p. 1088.
Vogt, M., Kunath, K., Dressman, J.B., 2008. Dissolution enhancement of fenofibrate by micronization, cogrinding, and spray-drying: comparison with commercial preparations. Eur. J. Pharm. Biopharm. 68, 283–288.
Wang, L., Cui, F.D., Sunada, H., 2006. Preparation and evaluation of solid dispersions of nitrendipine prepared with fine silica particles using melt mixing method. Chem. Pharm. Bull. 54, 37–43.
Wishart, D.S., Konx, C., Guo, A.C., Shrivastava, S., Hassanali, M., Stothard, P., Chang, Z., Woolsey, J., 2006. Drug bank: a comprehensive resource for in silico drug discovery and exploration. Nucleic Acids Res. 1, D668–D672.
Zhou, A., Zhang Geoff, G.Z., Law, D., Grant David, J.W., Schmitt, E.A., 2002. Physical stability of amorphous pharmaceuticals: importance of configurational thermodynamic quantities and molecular mobility. J. Pharm. Sci. 1, 1863–1872.